

Active vibration isolator based on micromachined electrostatic actuators

Chong Li¹ ✉, Haoyue Yang¹, Robert N. Dean², George T. Flowers¹

¹Department of Mechanical Engineering, Auburn University, Auburn, AL, 36830, USA

²Department of Electrical and Computer Engineering, Auburn University, Auburn, AL, 36830, USA

✉ E-mail: czl0047@auburn.edu

Published in Micro & Nano Letters; Received on 7th April 2016; Accepted on 15th July 2016

Parallel plate actuators (PPAs) are widely used actuators in microelectromechanical systems. A PPA can be utilised as a passive/active vibration isolator. A novel active vibration isolator with a simple structure, which requires a constant voltage source and series capacitor, is proposed. The principle of the spring softening effect is analysed, which can avoid a specific external disturbance by changing its resonant frequency. A simulation study was performed to verify the feasibility of this type of isolator.

1. Introduction: Several types of microdevices are adversely affected by high-frequency mechanical vibrations present in the operating environment [1, 2]. Examples include microelectromechanical systems (MEMS) vibratory gyroscopes and resonators [3] and microoptics [4]. Various types of MEMS vibration isolators have been developed for use in the packaging of these vibration sensitive devices. Passive isolators consist of a spring–mass–damper MEMS device and usually have a very high mechanical quality factor, which makes them susceptible to ring at the isolator’s resonant frequency. Active isolators have been realised by using state sensing of the proof mass motion and feeding one or more of these states back through an actuator to adjust the frequency response of the isolator. For example, the technique known as skyhook damping uses velocity feedback to adjust, and typically increase, the damping of the isolator. Although these techniques are doable, they require state sensing or state estimation, with feedback electronics to drive the actuator.

A simpler MEMS active vibration isolator architecture employs only a parallel plate actuator (PPA) with the MEMS spring–mass–damper structure. The PPA driven with a DC voltage, in its stable operating range, displaces the proof mass, which results in a change in the effective system spring constant due to the electrostatic spring softening effect. This results in a change in the resonant frequency and the quality factor of the isolator. However, due to the nonlinearities inherent in this type of device, the stable operating range is reduced as the PPA voltage is increased. Furthermore, even when the isolator is stable in steady state, a sufficiently large transient response can also drive it into the unstable regime, resulting in the electrodes snapping into contact.

In this Letter, the PPA-based active vibration isolator is developed and its performance is evaluated. The characteristics of the

transient instability are investigated and its stable range of operation is specified, for external disturbances. This MEMS PPA-based active vibration isolator can improve performance compared with passive isolators, while being much simpler than state feedback active isolators.

2. Kinematics of PPAs: Fig. 1 demonstrates the operational principle of a PPA. A PPA has two planar electrodes that arranged in parallel configuration. One electrode is fixed and the other one is movable which is suspended with a spring, whose stiffness is defined as k . The two electrodes have an overlapping area, A , and an initial gap between them of x_0 . The capacitance between the two electrodes, C_{act} , is defined as

$$C_{act} = \frac{\epsilon_0 \epsilon_r A}{x_0 - x}; \quad (1)$$

when the movable electrode is located in its initial position, the capacitance between the two electrodes obtains a minimum value C_m

$$C_m = \frac{\epsilon_0 \epsilon_r A}{x_0}, \quad (2)$$

where ϵ_0 is the permittivity of the vacuum, ϵ_r is the relative permittivity of the material in between the electrodes and x is the displacement of the movable electrode. An electrostatic force will be generated if a voltage, V_{act} , is applied across the movable and fixed electrode, which can be modelled as

$$F_e(x, V_{act}) = \frac{\epsilon_0 \epsilon_r A V_{act}^2}{2(x_0 - x)^2}. \quad (3)$$

The electrostatic force drives the movable electrode toward the fixed electrode until the net force is zero

$$F_e(x, V_{act}) = F_s, \quad (4)$$

where F_s is the spring force

$$F_s = kx \quad (5)$$

from the mechanical suspension system. In this simplified PPA model, the stiffness of the spring is assumed to be satisfactorily modelled by a spring constant. Additionally, when the electrode

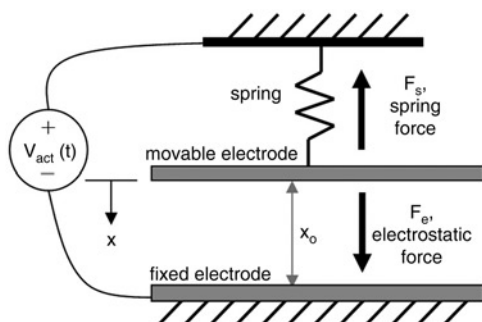


Fig. 1 Illustration of an electrostatic PPA

overlap area A is much greater than the initial gap x_0 , the capacitive fringing field effects can be ignored [5]. On the basis of (3), a nonlinear differential equation can be derived to describe the kinematics of the PPA

$$m\ddot{x} = -c\dot{x} - kx + \frac{\epsilon_0\epsilon_rAV_{act}^2}{2(x_0 - x)^2}. \quad (6)$$

Here c is the damping coefficient of the system and m is the proof mass of the movable electrode. The mechanical quality factor, Q , is

$$Q = \frac{\omega_0 m}{c}. \quad (7)$$

Most of the MEMS devices are designed to be lightly damped with high Q [5, 6], except MEMS accelerometers, which tend to be designed critically damped [7]. The mechanical natural frequency of the system, ω_0 , is

$$\omega_0 = \sqrt{\frac{k}{m}}. \quad (8)$$

The main drawback of the PPA is its limited stable travelling range, where $0 \leq x < x_0/3$. This is caused by the nonlinearity of the driving electrostatic force, while the spring force is linearly proportional to the displacement. Thus, the electrostatic force grows faster than the spring force when the displacement increases [8]. If the V_{act} attempts driving the movable electrode beyond one third of x_0 , the electrostatic force is always greater than the spring force, then the net force cannot reach to an equilibrium. This results in the two electrodes snapping into contact, which is also called snap-in effect. The minimum value of the voltage that will cause the snap-in effect is referred to as the pull-in voltage, V_{pi} , where

$$V_{pi} = \sqrt{\frac{8(x_0)^3}{27\epsilon_0\epsilon_rA}}. \quad (9)$$

3. Active vibration isolator using spring softening effect: The PPA can be utilised as a micromachined passive or active vibration isolator [9, 4] when the vibration sensitive microdevice can be mounted on the movable plate. The passive vibration isolator can reduce the influence of mechanical shock and high-frequency noise. The drawback of the passive isolator is that it is sensitive to external frequency components at the PPA's natural frequency and to fabrication tolerances [9]. To improve the performance when the external disturbance matches the isolator's natural frequency, an active vibration isolator was proposed by Kim *et al.* [4]. The active vibration isolator introduced additional damping force by using a velocity sensor and feedback electronics. The proposed novel active vibration isolator has a simple structure which is demonstrated in Fig. 2. The vibration sensitive device that is to be isolated is mounted on the PPA proof mass and a constant voltage is applied to the PPA.

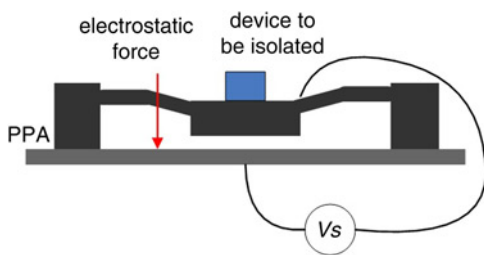


Fig. 2 Illustration of the active vibration isolator

Thus, the resonant frequency is changed due to the spring softening effect.

To explore the resonant frequency when the movable electrode is shifted by a constant voltage, a linear system analysis is performed where the system is linearised around an equilibrium point $(x_{1e}, 0, V_{ce})$ and $V_{ce} = V_s$

$$\delta\dot{x} = \begin{bmatrix} 0 & 1 \\ -\frac{k}{m} + \frac{\epsilon_0\epsilon_rAV_{ce}^2}{m(x_0 - x_{1e})^3} & -\frac{c}{m} \end{bmatrix} \delta x + \begin{bmatrix} 0 \\ \frac{\epsilon_0\epsilon_rAV_{ce}}{m(x_0 - x_{1e})^2} \end{bmatrix} \delta V_{ce}, \quad (10)$$

where

$$\delta x = x - x_{1e}, \quad (11)$$

$$\delta\dot{x} = \dot{x} \quad (12)$$

and

$$\delta V_{act} = V_{act} - V_{ce}. \quad (13)$$

In this case, the resonant frequency given in (5) becomes

$$\omega_{xe} = \sqrt{\frac{k}{m} - \frac{\epsilon_0\epsilon_rAV_{ce}^2}{m(x_0 - x_{1e})^3}}. \quad (14)$$

It is obvious that the resonant frequency is influenced by the constant input voltage V_{act} and its equilibrium point x_e . Thus, it is simple to adjust its resonant frequency by changing V_{act} to prevent external disturbances from matching its original natural frequency.

However, PPAs have a limited stable travelling range (less than one third of the initial gap x_0) [10]. If the external disturbance's amplitude is large, it may cause the two electrodes to snap to each other where they cannot be separated again. In this case, the vibration isolator has failed. So, a stabilisation method is necessary to make this isolator practical. The series capacitor method (SCM) is a classical solution to extend the PPA's stable travelling range. Fig. 3 demonstrates the active vibration isolator with a series capacitor, where C_s is no greater than one half of C_m , which is described by (2). Since C_s is usually a very small capacitor, it can often be fabricated as a MEMS structure on the same chip as the PPA vibration isolator.

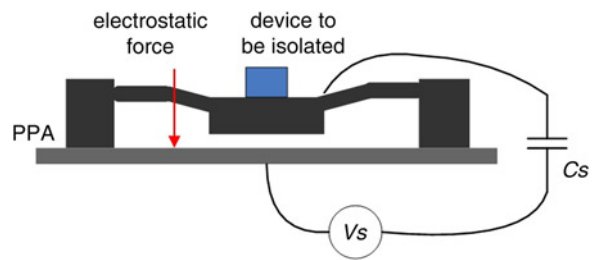


Fig. 3 Illustration of the active vibration isolator

Therefore, the linearised system around an equilibrium point $(x_{1e}, 0, V_{ce})$ and $V_{ce} = V_s$ is

$$\delta\dot{x} = \begin{bmatrix} 0 & 1 \\ -\frac{k}{m} + \frac{\epsilon_0\epsilon_rAV_{ce}^2}{m(3x_0 - x_{1e})^3} & -\frac{c}{m} \end{bmatrix} \delta x + \begin{bmatrix} 0 \\ \frac{\epsilon_0\epsilon_rAV_{ce}}{m(3x_0 - x_{1e})^2} \end{bmatrix} \delta V_{ce} \quad (15)$$

The resonant frequency ω_{xe} around this equilibrium point x_e is

$$\omega_{xe} = \sqrt{\frac{k}{m} - \frac{\epsilon_0\epsilon_rAV_{ce}^2}{m(3x_0 - x_{1e})^3}}. \quad (16)$$

The analytical results show that the isolator's resonant frequency can also be changed or tuned with the extended operational range.

4. Validation: A passive isolator chip is shown in Fig. 4 [9]. It can be made into an active isolator by using the bottom of the proof mass as the movable electrode of the PPA. The fabrication begins with a nominally 390 μm thick double side polished Si wafer. After cleaning, the wafer is thermally oxidised to grow $\sim 0.25 \mu\text{m}$ of SiO_2 using a wet oxidation process. Next, the SiO_2 on the front side of the wafer is patterned as required for metallisation. Then, the front side of the wafer is metallised with 800 A of Ti and 1500 A of Au by electron beam deposition. The metal layer is patterned to define all electrical traces and connection pads. A photoresist coating is applied to the front side and patterned for realising the spring elements. After photolithography, the exposed SiO_2 is removed by dry etching, and deep reactive ion etching (DRIE) is then used to etch 30 μm into the Si to define the thickness of the spring elements. The front side of the wafer is then cleaned. Next, the SiO_2 on the backside of the wafer is removed using buffered oxide etchant (BOE). After photolithography on the backside, the individual die is singulated and attached to a backing wafer. The exposed Si on the backside of the die are then DRIE etched to release the proof mass pad and spring elements on each die. Then, the die are removed from the backing wafer and cleaned. The vibration sensitive device requiring isolation is then attached to the proof mass pad of a fabricated isolator chip and wire bonded. The die is then placed in the desired chassis over a spacer to allow vertical motion of the proof mass structure. Finally, all external electrical connections are made to the isolator chip.

Simulation studies were performed to verify this technique by using MATLAB. The simulation used the parameters of the device shown in Fig. 4, which are given in Table 1.

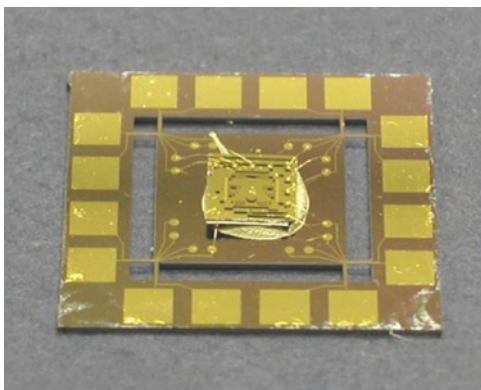


Fig. 4 Photograph of an MEMS gyroscope attached to the fabricated prototype vibration isolator [9]

Table 1 Parameters of the device

Symbol	Description	Value	Unit
k	spring constant	2880	N/m
c	damping coefficient	1.5×10^{-2}	N s/m
m	proof mass	96	μg
A	overlap area of the electrodes	10×10	μm^2
x_0	initial gap distance	10	μm
ϵ_0	permittivity of free space	8.854×10^{-12}	F/m
ϵ_r	permittivity of air	1.0006	N/A

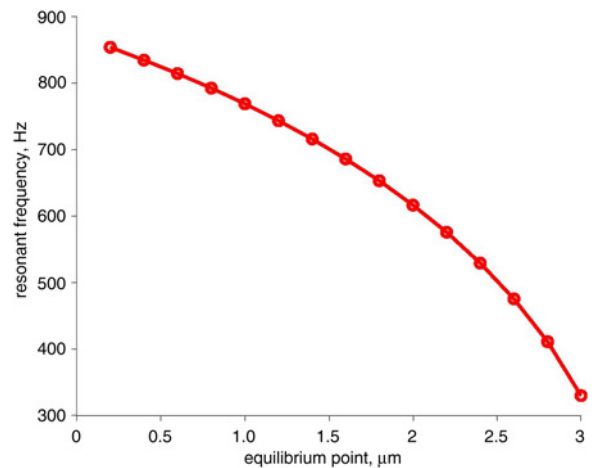


Fig. 5 Resonant frequencies at different equilibrium points of the active vibration isolator

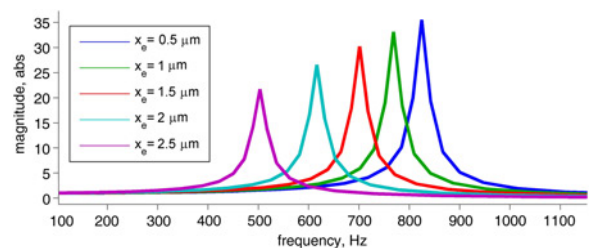


Fig. 6 Examples of frequency responses at different equilibrium points of the active vibration isolator

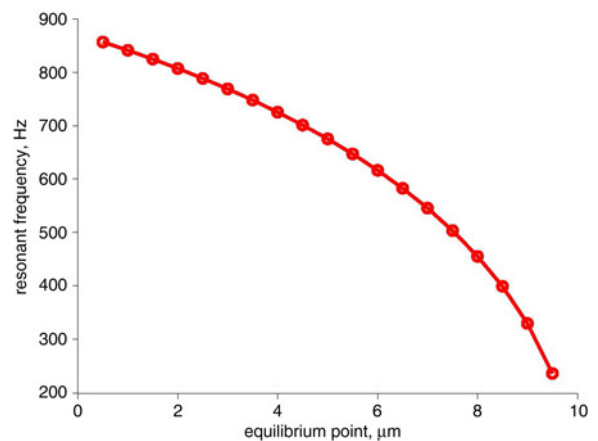


Fig. 7 Resonant frequencies in different equilibrium points of the active vibration isolator with SCM

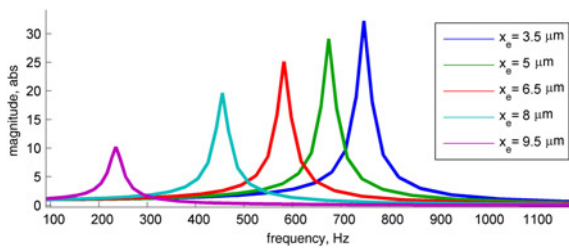


Fig. 8 Examples of frequency responses at different equilibrium points of the active vibration isolator with SCM

The resonant frequency changing effect of the standalone PPA was examined. Fig. 5 gives the values of resonant frequencies via changing the equilibrium point x_e from 0 to $1/3$ of x_0 , which was due to the changing of the input voltage V_{act} . It shows that the resonant frequency decreased from ~ 870 to 300 Hz. Fig. 6 gives examples of frequency responses with different equilibrium points. It further illustrates that different values of the voltage source can change the system's frequency characteristics.

Then, the frequency characteristics of the stabilised PPA were examined. Fig. 7 gives the values of resonant frequencies through the whole travelling range, which is due to the change of the input voltage V_{act} . Compared with the open loop operation, the variation of resonant frequency had a larger range which was between 220 and 870 Hz because the stable operation range was now larger. Fig. 8 gives examples of frequency response plots of the system with different equilibrium points. It illustrates the feasibility of the full range active vibration isolator using SCM.

5. Conclusions: The SCM-based MEMS vibration isolator has a simple structure which contains a PPA, a voltage source and a series capacitor. Its frequency characteristics can be changed by adjusting the voltage source, which can be utilised to tune the bandwidth of the vibration isolator over a wide range. Utilising the SCM method avoids issues with snap-in instability while increasing the tuning range. One application is

the selective filtering out of undesirable vibration components that would otherwise coincide with the high-Q isolator's resonant frequency.

6 References

- [1] Dean R.N., Anderson A., Reeves S.J., *ET AL.*: 'Electrical noise in MEMS capacitive elements resulting from environmental mechanical vibrations in harsh environments', *IEEE Trans. Ind. Electron.*, 2011, **58**, (7), pp. 2697–2705
- [2] Meyer Y., Cumunel G.: 'Active vibration isolation with a MEMS device effects of nonlinearities on control efficiency', *Smart Mater. Struct.*, 2015, **24**, (8), p. 085004
- [3] Kranz M.S., Hudson T.D., Ashley P.R., *ET AL.*: 'Single-layer silicon on-insulator MEMS gyroscope for wide dynamic range and harsh environment applications'. Micromachining and Microfabrication, Int. Society for Optics and Photonics, 2001, pp. 5–16
- [4] Kim S.J., Dean R., Flowers G., *ET AL.*: 'Active vibration control and isolation for micromachined devices', *J. Mech. Des.*, 2009, **131**, (9), p. 091002
- [5] Hosseini M., Zhu G., Peter Y.-A.: 'A new formulation of fringing capacitance and its application to the control of parallel-plate electrostatic micro actuators', *Analog Integr. Circuits Signal Process.*, 2007, **53**, (2-3), pp. 119–128
- [6] Pelliccia L., Cacciamani F., Farinelli P., *ET AL.*: 'High-tunable waveguide filters using ohmic RF MEMS switches', *IEEE Trans. Microw. Theory Tech.*, 2015, **63**, (10), pp. 3381–3390
- [7] Duwel A., Weinstein M., Gorman J., *ET AL.*: 'Quality factors of MEMS gyros and the role of thermoelastic damping'. Fifteenth IEEE Int. Conf. on Micro Electro Mechanical Systems, 2002, 2002, pp. 214–219
- [8] Li C., Dean R.N., Flowers G.T.: 'Analysis and dynamic simulation of the synthetic voltage division controller for extending the parallel plate actuator stable range of motion', *Microsyst. Technol.*, 2016, pp. 1–6
- [9] Dean R., Flowers G., Sanders N., *ET AL.*: 'Micromachined vibration isolation filters to enhance packaging for mechanically harsh environments', *J. Microelectron. Electron. Packag.*, 2005, **2**, (4), pp. 223–231
- [10] Moreira E., Alves F., Dias R., *ET AL.*: 'Bi-directional extended range parallel plate electrostatic actuator based on feedback linearization'. 2015 28th IEEE Int. Conf. on Micro Electro Mechanical Systems (MEMS), 2015, pp. 1036–1039